

## Heat Transfer Analysis of Casson Fluid Flow Over a Stretching Sheet with Radiative and Dissipative Effects and Variable Thermal Properties

P. M. Jadhav\*, A. B. Kulkarni, C. R. Hiremath

\* Department of Mathematics, Rani Channamma University, Belagavi, Karnataka, India  
 Department of Mathematics, Gogte College of Commerce, Belagavi, Karnataka, India  
 Department of Mechanical Engineering, Jain College of Engineering, Belagavi, Karnataka, India

### ABSTRACT

The main objective of the present paper is to study the unsteady free convection two-dimensional flow of a non-Newtonian Casson fluid with heat transfer analysis. In momentum transfer flow study is considered with suction/blowing.

The heat transfer study includes the influence of viscous dissipation, internal heat generation and thermal radiation with variable thermal conductivity. The governing modeled boundary layer partial differential equations are transformed into ordinary differential equations by suitable Similarity transformations. Further resultant equations are solved numerically using Matlab 45 Solver Via shooting technique. Various velocity and temperature profiles are investigated for governing flow and heat transfer parameters such as Suction, blowing, impermeability, unsteady parameter, casson parameter, convection parameter, Prandtl number, thermal conductivity parameter, radiation parameter, heat source/sink parameter, Eckert number etc. Also shear stress and the rate of heat transfer are studied and derived interms skin-friction co-efficient and Nusselt number. All the above investigations are displayed through graphs and the results are well in agreement with the published results.

**KEYWORDS:** Casson fluid, variable thermal conductivity, viscous dissipation, suction, unsteadyness and radiation.

### Nomenclature:

a,b,c constants  
 $C_f$  local skin-friction coefficient  
 $C_p$  specific heat at constant pressure  
 $Ec$  Eckert number  
 $V_w$  dimensionless suction velocity  
 $g$  acceleration due to gravity  
 $k^*$  absorption co-efficient  
 $R$  thermal radiation parameter  
 $N_u$  Nusselt number  
 $Pr$  Prandtl number  
 $q_r$  radiative heat flux in the y- direction  
 $R_e$  local Reynolds number  
 $Q_0$  Heat source/sink parameter  
 $T$  fluid temperature  
 $T_\infty$  ambient, temperature  
 $T_w$  stretching sheet temperature  
 $\beta$  casson parameter  
 $\beta^*$  coefficient of thermal expansion  
 $\epsilon$  variable thermal conductivity parameter  
 $K(T)$  variable thermal conductivity  
 $\mu$  dynamic viscosity  
 $\eta$  similarity variable  
 $\psi$  stream function  
 $\nu$  kinematic viscosity  
 $\rho$  density of the fluid  
 $\sigma^*$  Stefan Boltzman constant

## INTRODUCTION

Boundary layer flow of non-Newtonian behavior of casson fluid is studied through Navier-Stokes equations has become one of the good Research area in the present scenario and also in convective heat transfer. The wide range of applications of non-Newtonian property of the fluid receives an attention in many researchers, Scientists, Engineers, Mathematicians and Physicists to extend their ideas to contribute extensively more for future generation to enhance more comfort in all areas. Some of the examples of Non-Newtonian fluids in engineering and industrial process are blood plasma, food stuff processing, clay coating, paints, oil, greases, chocolate, mustard mayonnaise, shampoo, tooth paste. They are also used in industrials, metallurgy industries and polymer productions and extruction of polymers and Rubber sheets, hot rolling, melt spinning, paper coating manufacturing, wire drawing, glass fiber, microchip production, transpiration cooling, reactor fluidization, heat exchange equipments etc. the quality of output of final production totally depends on the rate of heat transfer. Considering this, gaining of knowledge of heat flow in boundary layer in all aspect of thermal condition are essential in convective heat transform. Many researchers are widely contributed their work in the field of Newtonian boundary layer flow with heat transfer studies.

The following investigations are mainly considered to contribute more in the wide area of non-Newtonian characteristics. Grubka and Bobba [1] studied the Heat transfer characteristics of a continuous stretching surface with variable temperature. Ali [2] discussed the Heat Transfer characteristics of a continuous stretching surface. Nagarani et al [3] studied the Exact Analysis Of Unsteady convective diffusion in casson fluid flow in an annulus – application to catheterized artery. Attia and Ahmed [4] investigated the Transient MHD couette flow of a casson fluid between parallel plates with heat transfer and used finite difference method to solve the governing differential equations. Pal and Hiremath [5] presented computational modeling of heat transfer over an unsteady stretching surface embedded in a porous medium. Ahmed et al.[6] expressed the results on time dependent pressure gradient effect on unsteady MHD couette flow and heat transfer of a casson fluid and used Crank –Nicolson method to obtain the result. Hayat et al [7] discussed Mass transfer effects on the unsteady flow of UCM fluid over a stretching sheet. Hayat et al [8] studied Soret and Dufour effects on magneto hydrodynamic (MHD) flow of a casson fluid. Vajravelu [9] investigated the Unsteady convective boundary layer flow of a viscous fluid at a vertical surface with variable fluid properties. Bhattacharyya[10] worked on MHD stagnation-point flow of casson fluid and heat transfer over a stretching sheet with thermal radiation. Mukhopadhyay et al [11] discussed about the Casson fluid flow over an unsteady stretching surface. Mukhopadhyay [12] presented Effects of thermal radiation on casson fluid flow and heat transfer over an unsteady stretching surface subjected to suction/blowing. Hussanian et al [13] have presented Unsteady boundary layer flow and heat transfer of a casson fluid past an oscillating vertical plate with newtonian heating. Castro et al [14] have worked on Unsteady wall shear stress analysis from image based computational fluid dynamic aneurysm models under newtonian and casson rheological models. Elbashbeshy and Bazid [15] studied about Heat transfer over an unsteady stretching surface. Khalid et al [16] discussed Exact solutions for unsteady free convection flow of casson fluid over an oscillating vertical plate with constant wall temperature. Sumalatha and Bandari [17] have proposed an analyzing on Effects of radiation and heat source/sink on the flow of casson fluid over nonlinear stretching sheet. Megahed [18] worked on the Effect of slip velocity on casson thin film flow and heat transfer due to an unsteady stretching sheet in the presence of variable heat flux and viscous dissipation. Kirubhashankar et al [19] investigated the Casson fluid flow and heat transfer over an unsteady porous stretching surface . Khalid et al [20] studied the Exact solutions for unsteady free convection flow of casson fluid over an oscillating vertical plate with constant wall temperature. Reddy [21] discussed an unsteady radiative-convective boundary-layer flow of a casson fluid with variable thermal conductivity. Kumar and Gangadhar [22] presented the effect of chemical reactive species on slip flow of mhd casson fluid over a stretching sheet with heat and mass transfer. Heat transfer and flow of a casson fluid due to a stretching cylinder with the soret and dufour effects was investigated by Mahdy [23]. Hussain [24] proposed work on Flow of casson nanofluid with viscous dissipation and convective conditions. Effects of radiation on MHD free convection of a casson fluid from a horizontal circular cylinder with partial slip in non-Darcy porous medium with viscous dissipation was analyzed by Makanda et al [25]. Ahmed and Dutta [26] investigated the heat transfer in an unsteady MHD flow through an infinite annulus with radiation. Kuppala et al [27] worked on unsteady MHD convective heat and mass transfer of a casson fluid past a semi infinite vertical permeable moving plate with heat source/sink. Imran et al [28] studied the effects of slip on free convection flow of casson fluid over an oscillating vertical plate. The effect of thermal conductivity of viscous fluid on unsteady flow and heat transfer are analysed by Vajravelu et al [9]. Recently Reddy [21] examined the unsteady heat and flow transfer of a casson fluid.

Motivated by all the above analyzed investigations in the literature of non-Newtonian flow and heat transfer now in present study, The radiative convection of an unsteady flow and heat transfer of a casson fluid with variable thermal conductivity, viscous dissipation and heat source/ sink past a stretching sheet is considered.

**MATHEMATICAL FORMULATION**

The unsteady laminar boundary layer of two dimensional convective flow of a casson fluid and heat transfer is considered with plane  $x = 0$ . The unsteady fluid flow and heat transfer starts at  $t=0$  and  $x$ -axis moving along the sheet in the right direction.

The rheological equation of state of the flow of an isotropic incompressible Casson fluid is

$$\tau_{ij} = \begin{cases} 2\left(\mu_B + \frac{P_y}{\sqrt{2\pi}}\right)e_{ij}, \pi > \pi_c \\ 2\left(\mu_B + \frac{P_y}{\sqrt{2\pi_c}}\right)e_{ij}, \pi < \pi_c \end{cases} \tag{1a}$$

$$\tau = \tau_0 + \mu\dot{\sigma} \tag{1b}$$

Where  $\tau$  is the shear stress,  $\tau_0$  is the casson yield stress,  $\mu$  is the dynamic viscosity,  $\dot{\sigma}$  is the shear rate,  $\pi = e_{ij}e_{ij}$  and  $e_{ij}$  is the  $(i, j)^{th}$  component of the deformation rate,  $\pi_c$  is the double component of deformation rate,  $\pi_c$  is critical value of this double based on the non-Newtonian model,  $\mu_B$  is the plastic dynamic viscosity of the non-Newtonian fluid,  $P_y$  is the yield stress of the fluid there fore when the shear stress is smaller then the yield stress  $P_y$ , fluid exhibits no motion i,e it acts like a solid and it represents flow characteristics only when shear stress is greater then  $P_y$  and non-uniform velocity of the flow  $U_w(x, t) = \frac{cx}{1-\alpha t}$  with  $c > 0$  and  $\alpha \geq 0$  are constants with dimensions  $[time^{-1}]$  and initial stretching rate is  $c$ .

The governing equations of such type of flow of velocity field and temperature field with respect to time are as follows,

$$\frac{\partial u}{\partial x} + \frac{\partial v}{\partial y} = 0 \tag{2}$$

$$\frac{\partial u}{\partial t} + u \frac{\partial u}{\partial x} + v \frac{\partial v}{\partial y} = \nu \left(1 + \frac{1}{\beta}\right) \frac{\partial^2 u}{\partial y^2} + g\beta(T - T_\infty) \tag{3}$$

$$\frac{\partial T}{\partial t} + u \frac{\partial T}{\partial x} + v \frac{\partial T}{\partial y} = \frac{\partial}{\partial y} \left( K(T) \frac{\partial T}{\partial y} \right) - \frac{1}{\rho c_p} \frac{\partial q_r}{\partial y} + \mu \left( \frac{\partial u}{\partial y} \right)^2 + \frac{Q_0}{\rho c_p} (T - T_\infty) \tag{4}$$

Where  $u$  and  $v$  are the velocity components along  $x$  and  $y$  axis directions,  $t$  is the time variable,  $\nu$  is the kinematic viscosity,  $\beta = \frac{\mu_B}{P_y} \sqrt{2\pi_c}$  is the casson parameter of casson fluid,  $g$  is the acceleration due to gravity,  $\beta^*$  is the coefficient of thermal expansion,  $T$  is the fluid Temperature,  $T_\infty$  is the ambient temperature,  $\rho$  is the fluid Density,  $C_p$  is the Specific heat at constant pressure,  $\mu$  is the effective dynamic viscosity,  $K(T)$  is the variable thermal conductivity,  $q_r$  is the radiation heat flux and the expression for thermal conductivity assumed here is varying timely with temperature and is expressed as

$$\kappa(T) = k_\infty \left( 1 + \frac{\mathcal{E}}{\Delta T} (T - T_\infty) \right) \tag{5}$$

Where  $\Delta T = (T_w - T_\infty)$ ,  $T_w$  is the surface temperature,  $\mathcal{E}$  is the variable thermal conductivity parameter,  $k_\infty$  is the thermal conductivity of the fluid far away from the sheet. By Rosseland approximation, the radiative heat flux is expressed as

$$q_r = \frac{-4\sigma^*}{3k^*} \frac{\partial T^4}{\partial y} \tag{6}$$

where  $\sigma^*$  is the Stefan Boltzman constant and  $k^*$  is the absorption coefficient. Assuming the temperature difference within the flow in such a way that  $T^4$  is expressed in Taylor's series expansion about  $T_\infty$  and neglecting higher order terms we have

$$T^4 = 4T_\infty^3 T - 3T_\infty^4 \tag{7}$$

And by the consequence of equations (6) and (7), equation (4) can be converted to

$$\frac{\partial T}{\partial t} + u \frac{\partial T}{\partial x} + v \frac{\partial T}{\partial y} = \left( \frac{k}{\rho c_p} + \frac{16\sigma^* T_\infty^3}{3\rho c_p k^*} \right) \frac{\partial^2 T}{\partial y^2} + \mu \left( \frac{\partial u}{\partial y} \right)^2 + \frac{Q_0}{\rho c_p} (T - T_\infty) \tag{8}$$

With respect to boundary conditions for the flow and heat fields as

$$\begin{aligned} u &= U(x,t), v = V_w(t), T = T_w(x,t), \text{ at } y = 0 \\ u &\rightarrow 0, T \rightarrow T_\infty, \text{ as } y \rightarrow \infty \end{aligned} \tag{9}$$

Where  $V_w = -\frac{V_0}{1-\alpha t}$  is the suction/injection velocity of the fluid,  $T_w(x,t) = T_\infty + \frac{cx^2 T_0 (1-\alpha t)^{-3/2}}{2\nu}$  and

these are chosen to obtain new similarity transformations and it has significant role in converting governing partial differential equations (3) and (8) into ordinary differential equations.

Defining similarity transformation variables as

$$\eta = \sqrt{\frac{a}{\nu(1-\alpha t)}} y, \psi(x,y) = \sqrt{\frac{a\nu}{1-\alpha t}} xf(\eta) \text{ and } \theta(\eta) = \frac{T - T_\infty}{T_w - T_\infty} \tag{10}$$

and dimensionless functions  $f$  and  $\theta$ .  $\psi(x,y,t)$  is the stream function defined as

$$u = \psi_y \text{ and } v = -\psi_x$$

The velocity components  $u$  and  $v$  identically satisfies the continuity equation (2).

Using boundary conditions (9) and (10) in (3) and (8), equations (3) and (8) convert to

$$\left( 1 + \frac{1}{\beta} \right) f''' + ff'' - (f')^2 - A \left( f' + \frac{1}{2} \eta f'' \right) + \lambda \theta = 0 \tag{11}$$

$$\frac{1}{Pr} \left( (1 + \varepsilon \theta + R) \theta' \right)^2 + f \theta' - f' \theta - \frac{A}{2} (\theta + \eta \theta') + Ec f'' + Q_0 \theta = 0 \tag{12}$$

Boundary conditions corresponding to the above non-linear differential equations convert to

$$\begin{aligned} f(0) &= V_w, f'(0) = 1, \theta(0) = 1 \\ f'(\infty) &\rightarrow 0, \theta(\infty) \rightarrow 0 \end{aligned} \tag{13}$$

Where  $A = \frac{c}{a}$  - is the unsteady parameter,  $\lambda$  - is the convection parameter and if  $\lambda < 0$  represents opposing

flow and  $\lambda > 0$  is assisting flow,  $\lambda = 0$  forced convection flow,  $Pr = \frac{\nu}{\alpha}$  - Prandtl number,  $\varepsilon$  is the variable

thermal conductivity parameter,  $R = \frac{16\sigma^* T_\infty^3}{3\rho c_p k^*}$  - thermal radiation parameter,  $Ec$  - is the Eckert number,  $Q_0$  - is

the Heat source / sink parameter and dash on exponent represents the differentiation with respect to  $\eta$

**SOME RESULTS CONNECTED WITH FLOW AND HEAT TRANSFER**

Case(i) Comparison values of Nusselt number  $\theta'(0)$  for  $A = 0, \beta \rightarrow \infty, \lambda = 0, Ec = 0, \varepsilon = 0, Pr = 1, Q_0 = 0, R = 0$  with previously published papers

Grubka and Bobba[1]	Ali[2]	Elbashbeshy and Bazid[15]	Pal and Hiremath[5]	Present results
1.00000	1.0054	0.999999	1.00000	1.000064

Case(ii) when  $A = 0, \beta \rightarrow \infty, \lambda = 0, V_w = 0$  equation (11) assumes the closed form solution of the type

$$f(\eta) = 1 - e^{-\eta}$$

and solution of equation (12) can be expressed in terms of Kummar’s function by Grubka and Bobba[1] as

$$\theta(\eta) = \frac{M(2, 1 + Pr, e^{-\eta} Pr)}{M(2, 1 + Pr, Pr)} e^{(1-\eta-e^{-\eta})Pr}$$

Case(iii) when  $A = 0, \lambda = 0$ , analytical solution of equation (11) is

$$f(\eta) = \left(1 + \frac{1}{\beta}\right)^{1/2} \left[ 1 - e^{\frac{-\eta}{\left(1 + \frac{1}{\beta}\right)^{1/2}}} \right]$$

**SKIN FRICTION COEFFICIENT**

The co-efficient of Skin friction is defined and derived as  $\tau_w = \mu \left(\frac{\partial u}{\partial y}\right)_{y=0}, C_f = \left(1 + \frac{1}{\beta}\right) \frac{\tau_w}{\rho U^2}$  and

$$C_f \sqrt{Re_x} = \left(1 + \frac{1}{\beta}\right) f''(0)$$

**LOCAL NUSSELT NUMBER**

The coefficient of heat transfer is defined and derived as  $Nu_x = \frac{xq_w}{k_\infty (T_w - T_\infty)}$

where  $q_w = -k_\infty \left(\frac{\partial T}{\partial y}\right)_{y=0}, \frac{Nu}{\sqrt{Re_x}} = -\theta'(0)$  is the dimensionless Nusselt number where

$Re_x = \frac{Ux}{\nu}$  is the Local Reynolds number.

**NUMERICAL SOLUTION**

Solution of flow and heat transfer of boundary value problem defined by the equation (11) and (12) subjected to the boundary conditions (13) are solved by inbuilt function ode45 of MATLAB software. Initially it is necessary to express boundary valued problem into initial valued problem by guessing the appropriate initial slopes for  $f''(0)$  and  $\theta'(0)$ . Further these coupled equations are expressed as a system of five first order ordinary differential equations. Further these system of equations are solved by MATLAB inbuilt command for solving initial valued problem along with shooting technique.

**RESULTS AND DISCUSSION**

To reveal the effect of various set of governing parameters of unsteady laminar boundary layer flow and heat transfer on casson fluid flow and to encounter the physics of the problem, various graphs of velocity and temperature distribution are presented in the presence of suction, blowing and impermeability conditions.

Fig(1) displays the effect of unsteady parameter A on velocity profile with different values of  $V_w$ (suction, injection and impermeability) and it is observed from the figure that velocity profile decreases with increasing values of A. Physically it results in the thickness of the velocity boundary layer near the wall.

In case of steady and unsteady velocity profile decreases with respect to increasing values of Casson parameter  $\beta$  as expressed in the figure(2). Physically, it means that increasing values of  $\beta$  fluid yield stress decreases which cause a production for the resistance forces which makes the fluid velocity to decrease.

Figure(3) depicts the influence of convective parameter  $\lambda$  on longitudinal velocity  $f'(\eta)$  and it is clearly exhibits that as  $\lambda$  increases,  $f'(\eta)$  increase with the effect of suction, injection and impermeability.

The effect of unsteady parameter A on temperature profile is shown in figure(4). It shows from the figure that temperature profile decreases with increasing values of A. Physically it implies that as unsteady parameter increases there is a less heat transformed from fluid to sheet. For the steady flow, rate of cooling is very slow compared with unsteady that it will cool much faster.

Heat distribution of various values of Casson parameter  $\beta$  is drawn in figure(5) which exhibits the fact that for increasing values of  $\beta$  temperature profile decreases. To examine the physics, thermal thin layer thickness decreases with increasing values of  $\beta$ .

Figure (6) presents the graph of temperature distribution for various values of convection parameter  $\lambda$  it is seen from the figure that thermal boundary layer increases by increasing  $\lambda$  values.

Temperature profile for various values of Prandtl number Pr is shown in figure(7) and one can see from the graph that temperature profile decreases on increasing the values of Pr and boundary layer thickness decreases. The thermal boundary layer thickness decreases much in case of suction comparing with blowing as Prandtl number increases and heat transfers from the surface to ambient fluid because of negative values of Nusselt number. The effect of Prandtl number is generally used to decrease the heat transfer i.e increasing the rate of cooling. For higher values of Pr thins the boundary layer and for lower values of Pr will possess higher thermal conductivity, i.e thicker the boundary layer.

The temperature distribution for different values of thermal conductivity parameter  $\varepsilon$  is shown in figure(8). Here also temperature profile is increasing for increasing values of  $\varepsilon$ . This is due to the assumption that temperature dependent thermal conductivity reduce the magnitude of transverse velocity by the quantity  $\frac{\partial}{\partial y}(K(T))$ .

For increasing values of radiation parameter R the thermal boundary layer increases and it is shown in figure(9). Its physical significance is that the thermal boundary layer thickness increases by increasing R. This is because of the fact that in the heat conduction equation the coefficient  $\frac{Pr}{(1 + \varepsilon\theta + R)}$  reduces as R increases and the radiative

heat flux  $\frac{\partial q_r}{\partial y}$  increases as  $K$  decreases which effects the rate of radiative heat transfer to increase.

Figure(10) shows the effect of different values of Heat source/sink parameter on temperature. It clearly seen from the figure that temperature profile increases with increasing values of  $Q_0$ . This is because of the fact that heat source accumulates more heat on the stretching sheet to increase  $Q_0$  and thermal boundary layer thickness increases or the absorption reduce the thermal boundary layer thickness for uniform( $Q_0 < 0$ ) and thickness increases monotonically for higher values of  $Q_0 > 0$ .

The influence of Eckert number Ec on  $\theta(\eta)$  is shown in the figure(11). It reveals from the figure that temperature increases by increasing the values of Ec. Physically this behavior is observed because in presence of viscous dissipation heat energy is stored in the fluid and there is more significant generation of heat along the sheet.

Figure(12) represents the local skin friction profiles  $-f''(0)$  v/s casson parameter  $\beta$  for different values of unsteady parameter  $A$  on observing, it is seen that  $-f''(0)$  decreases on increasing values of  $A$ .

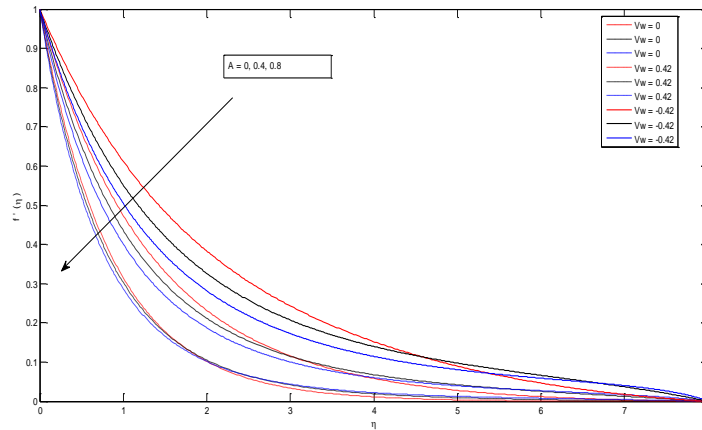
Figure(13) is plotted for local skin friction profile, on observing, skin friction profiles decrease as increasing in the parametric values of  $A$  with respect to  $\lambda$ . Figure(14) depicts  $-f''(0)$  v/s unsteady parameter  $A$  for different values of casson parameter  $\beta$  and it is decreasing by increasing values of  $\beta$ . The local skin friction co-efficient against  $\lambda$  with different values of casson parameter  $\beta$  is shown in figure(15), here also local skin friction co-efficient profiles decreases with increasing values of casson parameter  $\beta$ . Skin friction co-efficient distribution increases by increasing values of  $\lambda$  against unsteady parameter  $A$  is shown in figure(16).

In figure (17) the profiles of  $-f''(0)$  are drawn v/s casson parameter  $\beta$  with different vales of  $\lambda$ , it is show from the figure that it increases by increasing values of  $\lambda$ . Figure (18) is plotted for rate of heat transfer co-efficient for different values of  $\lambda$  with respect to  $Ec$ , on observing local Nusselt number decreasing as increase in parametric values  $\lambda$ . In figure(19) the wall temperature gradient  $-\theta'(0)$  against heat source parameter  $Q$  with different values of convection parameter  $\lambda$  is drawn. It is revealed from the figure that rate of heat transfer decreases for increasing values of  $\lambda$ . The rate of heat transfer for different values of  $Ec$  v/s convection parameter  $\lambda$  is shown in figure(20) and it is noted from the graph that  $-\theta'(0)$  enhances by increasing the values of Eckert number  $Ec$ . Figure(21) depicts the wall temperature gradient against  $Q$  with various values of  $Ec$ , the same effect follows in this scenario also. The profiles for Nusselt number v/s  $\lambda$  for various values of  $Q$  and it is decreasing on increasing values of  $Q$  is shown in figure (22). Figure(23) expresses the graph of temperature gradient  $-\theta'(0)$  v/s Eckert number  $Ec$  with respect to  $Q$ . It is noted from the figure that Nusselt number decreases on increasing heat source/sink parameter values.

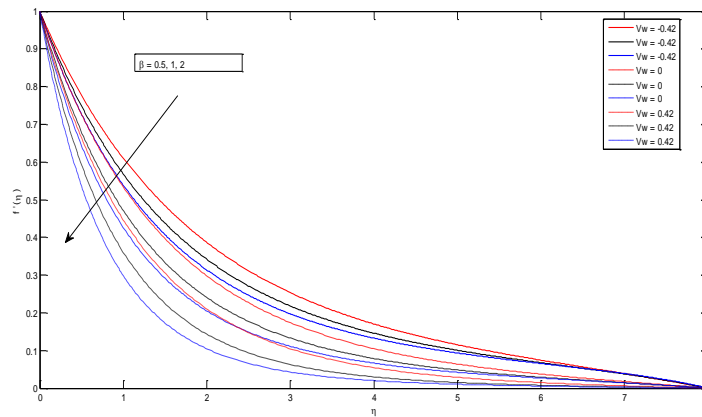
**REFERENCES**

- [1] Grubka LT, Bobba K M, Heat transfer characteristics of a continuous stretching surface with variable temperature. *Asme J. Heat Transfer* 107: (1985) 248-250
- [2] Ali M E, Heat Transfer characteristics of a continuous stretching surface, *Warme Stoffubertray* 29: (1994) 227-234
- [3] Nagarani, Deshmukhi, Sarojamma, Tirupati, and Jayaraman, Exact Analysis Of Unsteady convective diffusion in casson fluid flow in an annulus – application to catheterized artery *Acta Mechanica* 187, (2006) 189–202
- [4] Hazem Ali Attia, Mohamed Eissa Sayed-Ahmed, Transient MHD couette flow of a casson fluid between parallel plates with heat transfer, *Italian Journal Of Pure And Applied Mathematics* N. 27-2010 (19-38)
- [5] Pal And Hiremath, Computational modeling of heat transfer over an unsteady stretching surface embedded in a porous medium *Meccanica* 45: (2010)415-424
- [6] Sayed-Ahmed, Hazem A. Attia, Karem M. Ewis, Time dependent pressure gradient effect on unsteady mhd couette flow and heat transfer of a casson fluid *Scientific Research Engineering*, 2011, 3, 38-49
- [7] Hayat, Awais And Sajid, Mass transfer effects on the unsteady flow of ucm fluid over a stretching sheet . *International Journal Of Modern Physics B* Vol. 25, No. 21 (2011) 2863–2878
- [8] Hayat, Shehzad, Alsaedi, Soret and dufour effects on magnetohydrodynamic (MHD) flow of casson fluid *Appl. Math. Mech. -Engl. Ed.*, 33(10), (2012) 1301–1312
- [9] Vajravelu, Prasad and Chin-On Ng, Unsteady convective boundary layer flow of aviscous fluid at a verticalsurface with variable fluid properties. *Nonlinear analysis:Real world app.* 14(2013) 455-464.
- [10] Krishnendu Bhattacharyya, MHD stagnation-point flow of casson fluid and heat transfer over a stretching sheet with thermal radiation. *Hindawi Publishing Corporation Journal Of thermodynamics* Volume 2013, Article Id 169674, 9 Pages
- [11] Mukhopadhyay, Ranjan De and Battacharyya, Casson fluid flow over an unsteady stretching surface,

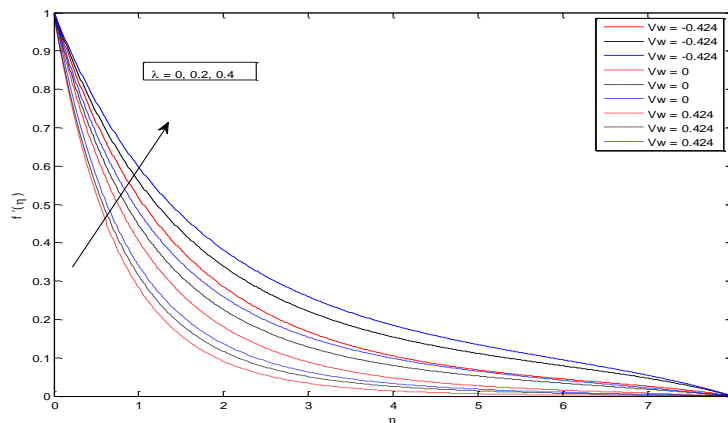
- Ain Shams.Eng.J, 4, (2013)933-938
- [12] Swati Mukhopadhyay, Effects of thermal radiation on casson fluid flow and heat transfer over an unsteady stretching surface subjected to suction/blowing  
Chin. Phys. B Vol. 22, No. 11 (2013) 114702
- [13] Abid Hussanan, Mohd Zuki Salleh, Razman Mat Tahar, Ilyas Khan, Unsteady boundary layer flow and heat transfer of a casson fluid past an oscillating vertical plate with newtonian heating  
Plos One 9(10): E108763. Doi:10.1371/Journal.Pone.0108763
- [14] Marcelo A. Castro, Maria C. Ahumada Olivares, Christopher M. Putman, Juan R. Cebral  
Unsteady wall shear stress analysis from image based computational fluid dynamic aneurysm models under newtonian and casson rheological models  
Med Biol Eng Comput (2014) 52:827–839
- [15] Elbashbeshy EMA, Bazid Maa, Heat transfer over an unsteady stretching surface  
Heat Mass Transf 41: (2004) 1-4
- [16] Khalid. A, Khan I., Shafic S., Exact solutions for unsteady free convection flow of casson fluid over an oscillating vertical plate with constant wall temperature,  
Abstr.Appl.Anal.2014, Article Id-946350 (2014)
- [17] Chenna Sumalatha, Shankar Bandari, Effects of radiations and heat source/sink on a casson fluid flow over nonlinear stretching sheet  
World Journal of Mechanics, 2015, 5, 257-265
- [18] Megahed, Effect of slip velocity on casson thin film flow and heat transfer due to unsteady stretching sheet in presence of variable heat flux and viscous dissipation  
Appl. Math. Mech. -Engl. Ed., 36(10), (2015)1273–1284
- [19] Kirubhashankar, S. Ganesh and Mohamed Ismail, Casson fluid flow and heat transfer over an unsteady porous stretching surface  
Applied Mathematical Sciences, Vol. 9, 2015, No. 7, 345 – 351
- [20] Asma Khalid, Ilyas Khan And Sharidan Shafie, Exact solutions for unsteady free convection flow of casson fluid over an oscillating vertical plate with constant wall temperature  
Hindawi Publishing Corporation Abstract And Applied Analysis Volume 2015, Article Id 946350, 8 Pages
- [21] Gnaneswara Reddy, Unsteady radiative-convective boundary-layer flow of a casson fluid with variable thermal conductivity  
Journal of Engineering Physics and Thermophysics, Vol. 88, No. 1, January, 2015
- [22] Sathies Kumar And K. Gangadhar, Effect of chemical reaction on slip flow of mhd casson fluid over a stretching sheet with heat and mass transfer  
Advances In Applied Science Research, 2015, 6(8):205-223
- [23] Mahdy, Heat transfer and flow of a casson fluid due to a stretching cylinder with the soret and dufour effects  
Journal Of Engineering Physics And Thermophysics, Vol. 88, No. 4, July, 2015
- [24] Hussain, Shehzad, Alsaedi, Hayat, and Ramzan, Flow of casson nanofluid with viscous dissipation and convective conditions: a mathematical model  
J. Cent. South Univ. (2015) 22: 1132–1140
- [25] Gilbert Makanda, Sachin Shaw And Precious Sibanda, Effects of radiation on mhd free convection of a casson fluid from a horizontal circular cylinder with partial slip in non-darcy porous medium with viscous dissipation  
Boundary Value Problems 2015:75
- [26] Ahmed N, Dutta M, Heat transfer in an unsteady MHD flow through an infinite annulus with radiation.  
Boundary Value Problems, 2015 Article Id 11
- [27] Sekhar Kuppala R, Viswanatha Reddy G, Murali Krishna Ch, Unsteady MHD convective heat and mass transfer of a casson fluid past a semi infinite vertical permeable moving plate with heat source/sink  
Global Journal Of Pure And Applied Mathematics (Gjpam) Issn 0973-1768 Volume 12,Number 1 (2016)
- [28] Muhammad A Imran, Shakila Sarwar And Muhammad Imran, Effects of slip on free convection flow of casson fluid over an oscillating vertical plate  
Boundary Value Problems 2016:30



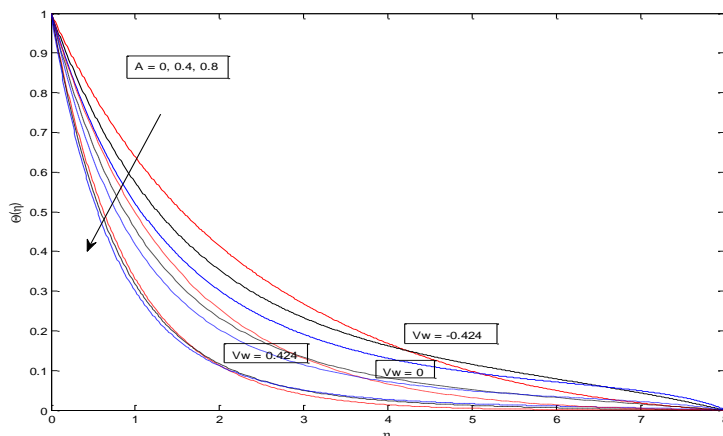
**Fig.1 Velocity distribution for different values of unsteady parameter A for various values of Suction parameter  $V_w$  with fixed values of  $Pr = 0.7$ ;  $\beta = 2$ ;  $\varepsilon = 0.2$ ;  $R = 0.1$ ;  $\lambda = 0.1$ ;  $Ec = 0.1$ ;  $Q = 0.4$ ;**



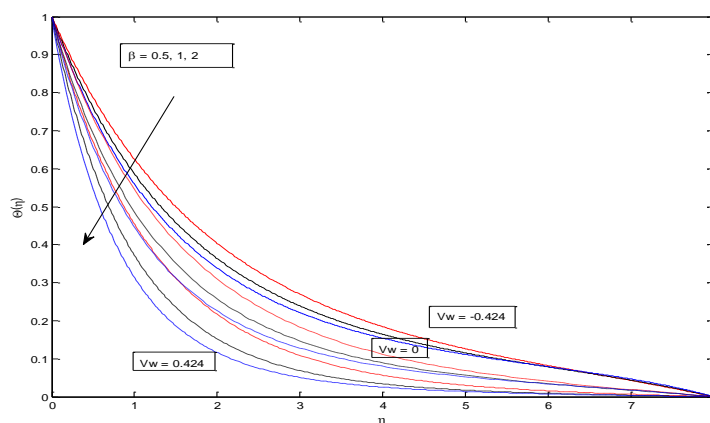
**Fig.2 Velocity distribution for different values of Casson parameter  $\beta$  for various values of Suction parameter  $V_w$  with fixed values of  $A = 0.5$ ;  $Pr = 0.7$ ;  $\varepsilon = 0.2$ ;  $R = 0.1$ ;  $\lambda = 0.1$ ;  $Ec = 0.1$ ;  $Q = 0.4$ ;**



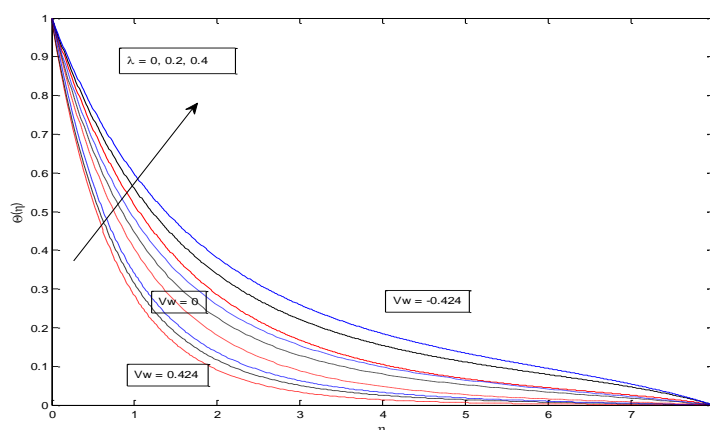
**Fig.3 Velocity distribution for different values of Convective parameter  $\lambda$  for various values of Suction parameter  $V_w$  with fixed values of  $A = 0.5$ ;  $Pr = 0.7$ ;  $\beta = 0.2$ ;  $\varepsilon = 0.2$ ;  $R = 0.1$ ;  $Ec = 0.1$ ;  $Q = 0.4$ ;**



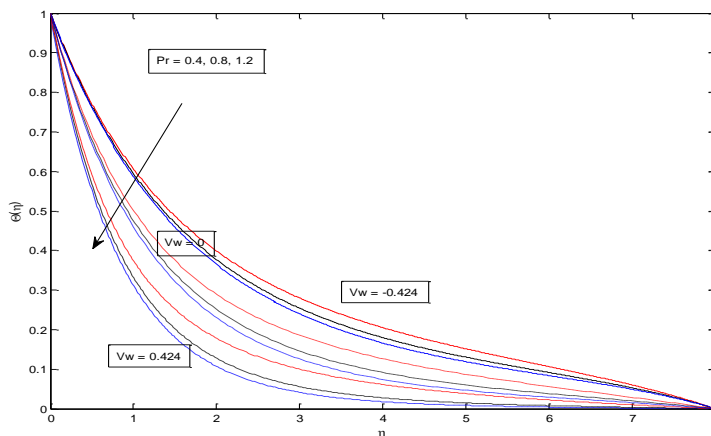
**Fig.4 Temperature distribution for different values of Unsteady parameter A for various values of Suction parameter Vw with fixed values of Pr = 0.7;  $\beta = 02$ ;  $\epsilon = 0.2$ ; R = 0.1;  $\lambda = 0.2$ ; Ec = 0.1; Q = 0.4;**



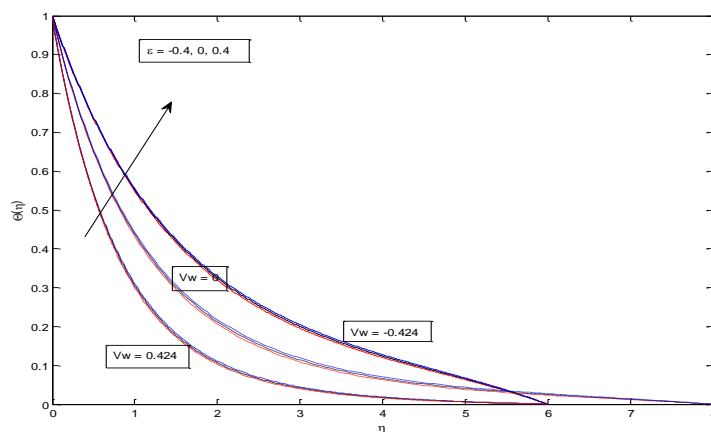
**Fig.5 Temperature distribution for different values of Casson parameter  $\beta$  for various values of Suction parameter Vw with fixed values of A = 0.5; Pr = 0.7;  $\epsilon = 0.2$ ; R = 0.1;  $\lambda = 0.2$ ; Ec = 0.1; Q = 0.4;**



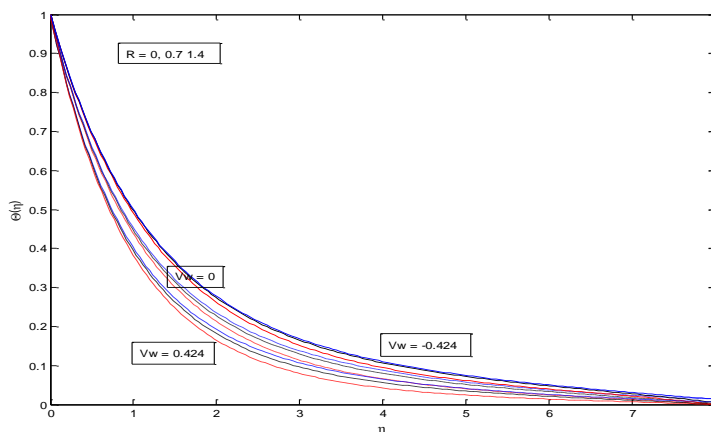
**Fig.6 Temperature distribution for different values of Convection parameter  $\lambda$  for various values of Suction parameter Vw with fixed values of A = 0.5; Pr = 0.7;  $\beta = 02$ ;  $\epsilon = 0.2$ ; R = 0.1; Ec = 0.1; Q = 0.4;**



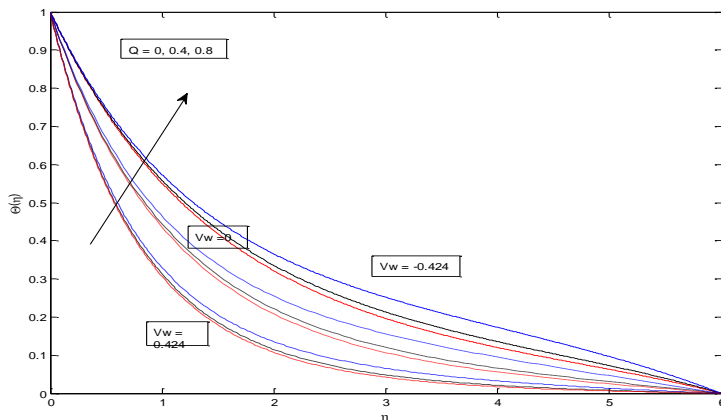
**Fig.7 Temperature distribution for different values of Prandtl number  $Pr$  for various values of Suction parameter  $V_w$  with fixed values of  $A = 0.5$ ;  $\beta = 0.2$ ;  $\varepsilon = 0.2$ ;  $R = 0.1$ ;  $\lambda = 0.4$ ;  $Ec = 0.1$ ;  $Q = 0.4$ ;**



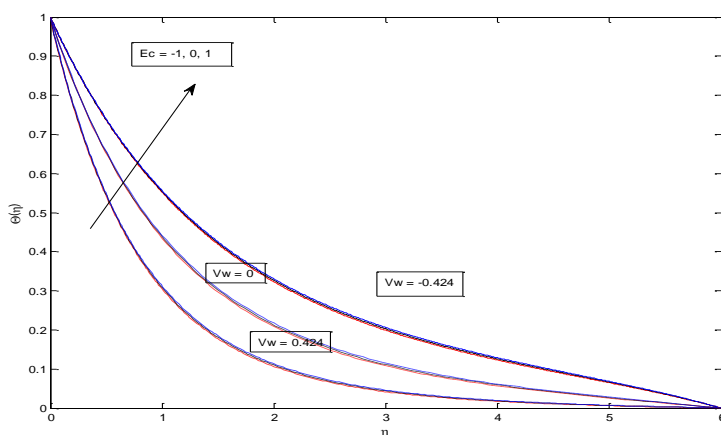
**Fig.8 Temperature distribution for different values of Thermal conductivity parameter  $\varepsilon$  for various values of Suction parameter  $V_w$  with fixed values of  $A = 0.5$ ;  $Pr = 0.7$ ;  $\beta = 0.2$ ;  $R = 0.1$ ;  $\lambda = 0.2$ ;  $Ec = 0.1$ ;  $Q = 0.2$ ;**



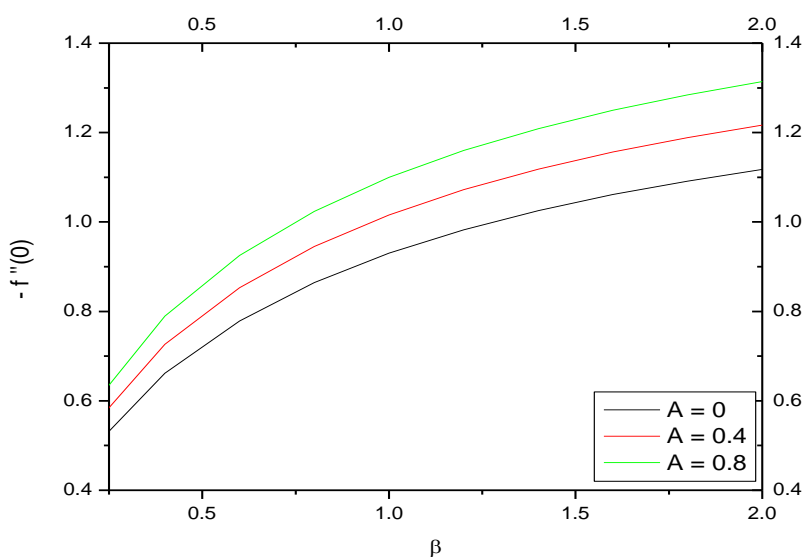
**Fig.9 Temperature distribution for different values of Radiation parameter  $R$  for various values of Suction parameter  $V_w$  with fixed values of  $A = 0.5$ ;  $Pr = 0.7$ ;  $\beta = 0.2$ ;  $\varepsilon = 0.2$ ;  $\lambda = 0.2$ ;  $Ec = 0.1$ ;  $Q = 0.2$ ;**



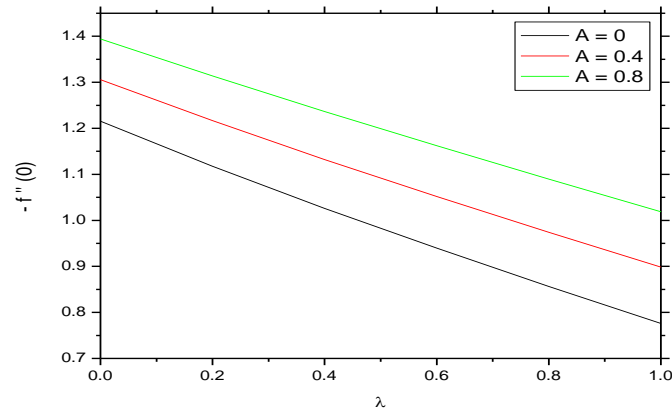
**Fig.10 Temperature distribution for different values of Heat Source/sink parameter  $Q$  for various values of Suction parameter  $V_w$  with fixed values of  $A = 0.5$ ;  $Pr = 0.7$ ;  $\beta = 0.2$ ;  $\epsilon = 0.1$ ;  $R = 0.2$ ;  $\lambda = 0.2$ ;  $Ec = 0.2$ ;**



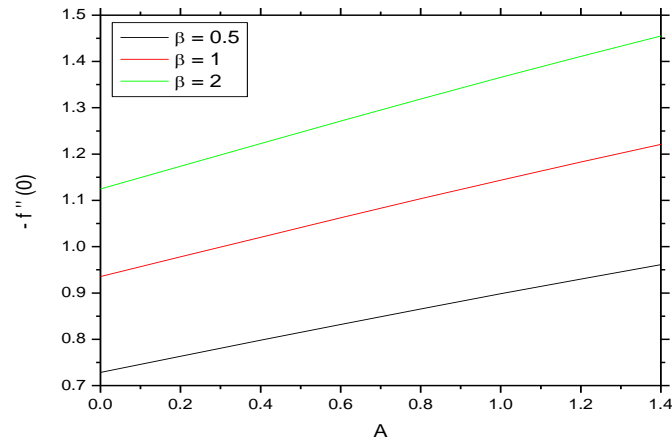
**Fig.11 Temperature distribution for different values of Eckert number  $Ec$  for various values of Suction parameter  $V_w$  with fixed values of  $A = 0.5$ ;  $Pr = 0.7$ ;  $\beta = 0.2$ ;  $\epsilon = 0.1$ ;  $R = 0.2$ ;  $\lambda = 0.2$ ;  $Q = 0.2$ ;**



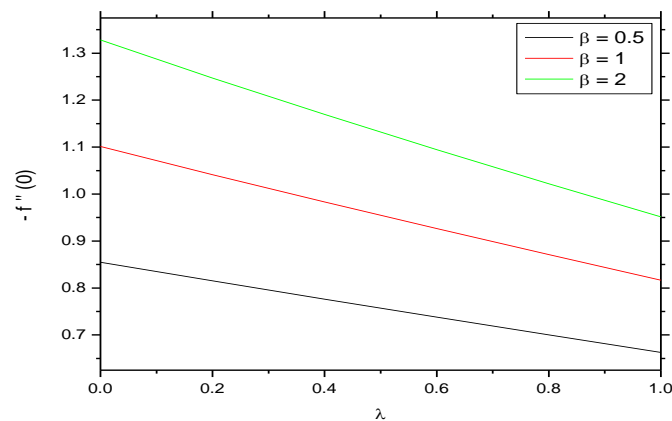
**Fig.12 Skin friction  $-f''(0)$  V/s Casson parameter  $\beta$  for different values of Unsteady parameter  $A$  with  $Pr = 0.7$ ;  $V_w = 0.424$ ;  $\epsilon = 0.1$ ;  $R = 0.2$ ;  $\lambda = 0.2$ ;  $Ec = 1$ ;  $Q = 0.2$ ;**



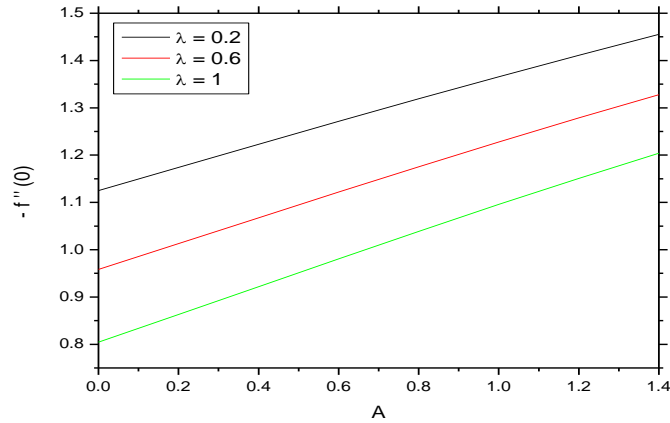
**Fig.13 Skin friction  $-f''(0)$  V/s Convective parameter  $\lambda$  for different values of Unsteady parameter  $A$  with  $Pr = 0.7$ ;  $\beta = 2$ ;  $\varepsilon = 0.1$ ;  $R = 0.2$ ;  $V_w = 0.424$ ;  $Ec = 01$ ;  $Q = 0.2$ ;**



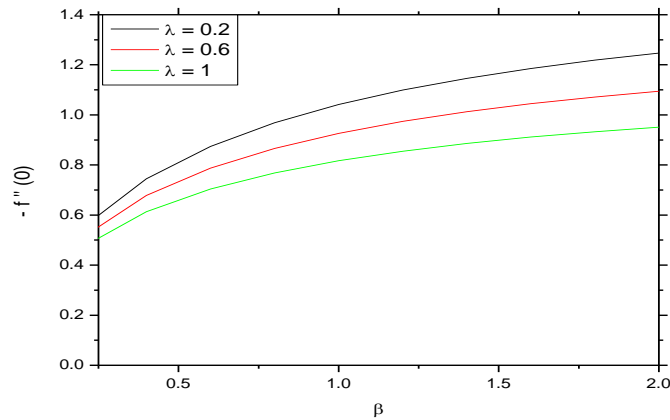
**Fig.14 Skin friction  $-f''(0)$  V/s Unsteady parameter  $A$  for different values of Casson parameter  $\beta$  with  $Pr = 0.7$ ;  $\varepsilon = 0.1$ ;  $R = 0.2$ ;  $\lambda = 0.2$ ;  $Ec = 0.2$ ;  $Q = 0.2$ ;  $V_w = 0.424$ ;**



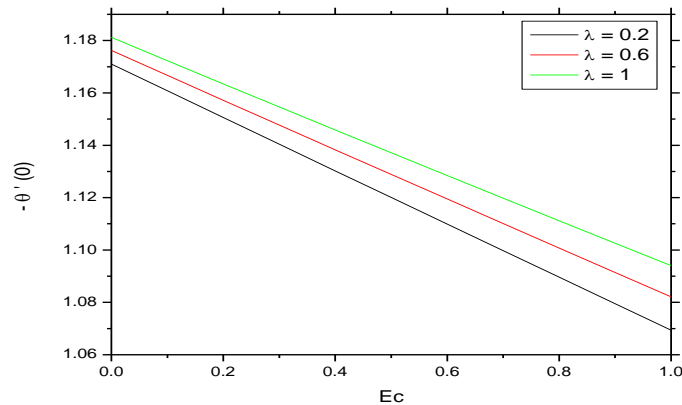
**Fig.15 Skin friction  $-f''(0)$  V/s Convective parameter  $\lambda$  for different values of Casson parameter  $\beta$  with  $A = 0.5$ ;  $Pr = 0.7$ ;  $\varepsilon = 0.1$ ;  $R = 0.2$ ;  $V_w = 0.424$ ;  $Ec = 0.2$ ;  $Q = 0.2$ ;**



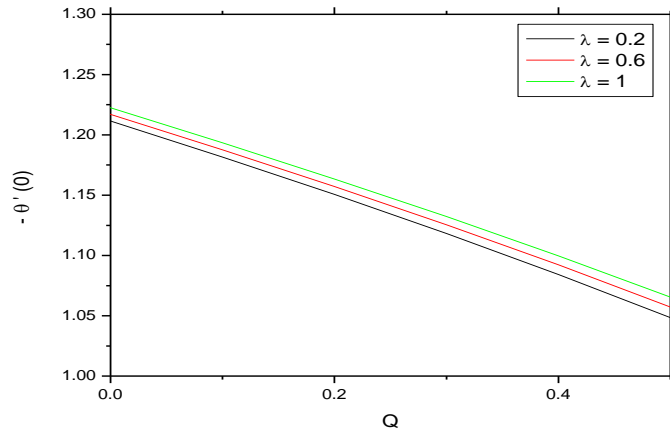
**Fig.16 Skin friction  $-f''(0)$  V/s Unsteady parameter A for different values of Convective parameter  $\lambda$  with  $V_w = 0.424$ ;  $Pr = 0.7$ ;  $\beta = 2$ ;  $\varepsilon = 0.1$ ;  $R = 0.2$ ;  $Ec = 0.2$ ;  $Q = 0.2$ ;**



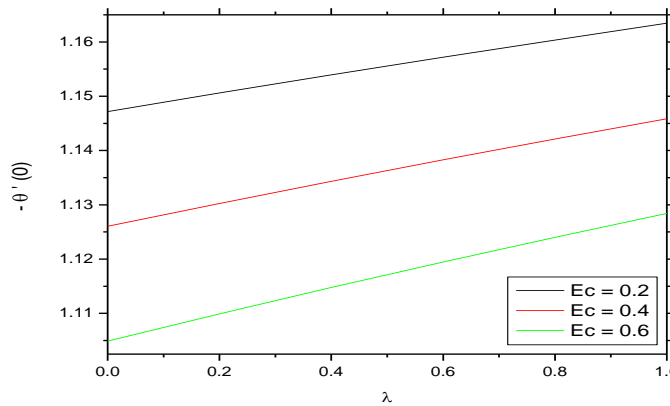
**Fig.17 Skin friction  $-f''(0)$  V/s Casson parameter  $\beta$  for different values of Convective parameter  $\lambda$  with  $A = 0.5$ ;  $Pr = 0.7$ ;  $V_w = 0.424$ ;  $\varepsilon = 0.1$ ;  $R = 0.2$ ;  $Ec = 0.2$ ;  $Q = 0.2$ ;**



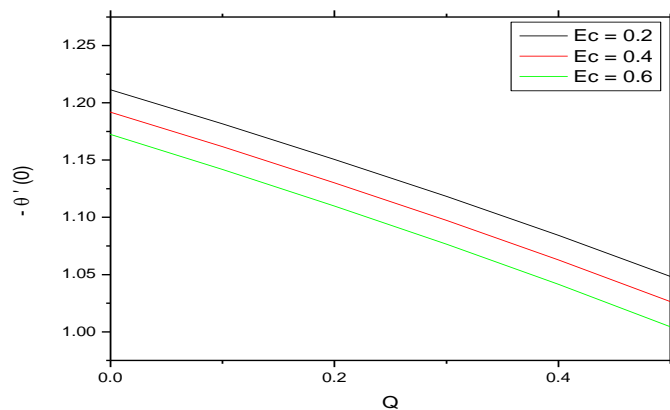
**Fig.18 Wall Temperature gradient  $-\theta'(0)$  V/s Eckert number  $Ec$  for different values of Convection Parameter  $\lambda$  with  $A = 0.5$ ;  $V_w = 0.424$ ;  $Pr = 0.7$ ;  $\beta = 0.2$ ;  $\varepsilon = 0.1$ ;  $R = 0.2$ ;  $Q = 0.2$ ;**



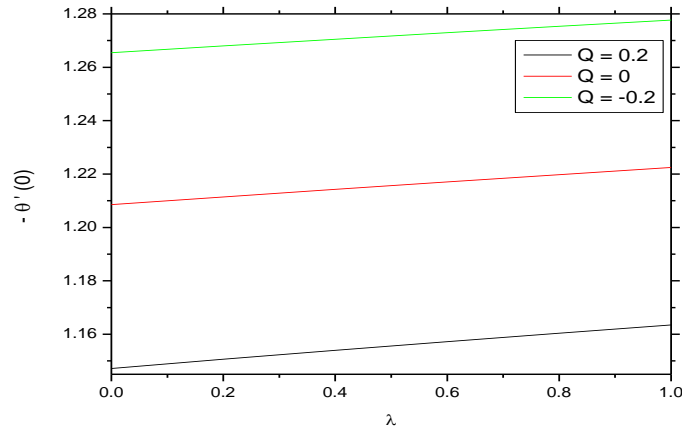
**Fig.19** Wall Temperature gradient  $-\theta'(0)$  V/s Heat Source/sink Parameter  $Q$  for different values of Convection Parameter  $\lambda$  with  $A = 0.5$ ;  $Pr = 0.7$ ;  $\beta = 0.2$ ;  $\varepsilon = 0.1$ ;  $R = 0.2$ ;  $Ec = 0.2$ ;  $V_w = 0.424$ ;



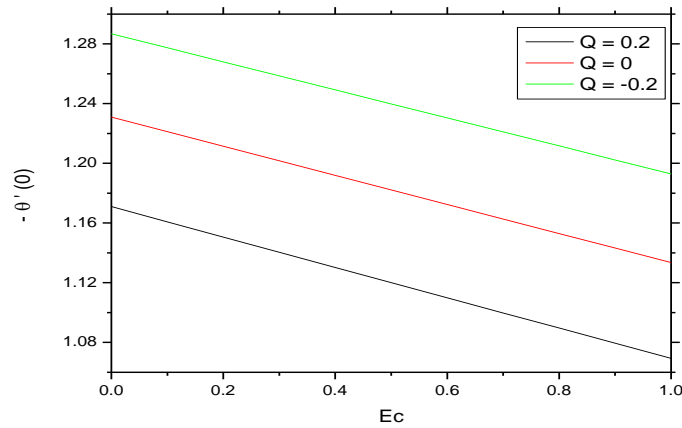
**Fig.20** Wall Temperature gradient  $-\theta'(0)$  V/s Convection Parameter  $\lambda$  for different values of Eckert number  $Ec$  with  $A = 0.5$ ;  $Pr = 0.7$ ;  $\beta = 0.2$ ;  $\varepsilon = 0.1$ ;  $R = 0.2$ ;  $V_w = 0.424$ ;  $Q = 0.2$ ;



**Fig.21** Wall Temperature gradient  $-\theta'(0)$  V/s Heat Source/sink Parameter  $Q$  for different values of Eckert number  $Ec$  with  $A = 0.5$ ;  $Pr = 0.7$ ;  $\beta = 0.2$ ;  $\varepsilon = 0.1$ ;  $R = 0.2$ ;  $\lambda = 0.2$ ;  $V_w = 0.424$ ;



**Fig.22 Wall Temperature gradient  $-\theta'(0)$  V/s Convection Parameter  $\lambda$  for different values of Heat Source/sink Parameter  $Q$  with  $A = 0.5$ ;  $Pr = 0.7$ ;  $\beta = 0.2$ ;  $\epsilon = 0.1$ ;  $R = 0.2$ ;  $Ec = 0.2$ ;  $V_w = 0.424$ ;**



**[29] Fig.23 Wall Temperature gradient  $-\theta'(0)$  V/s Eckert number  $Ec$  for different values of Heat Source/sink Parameter  $Q$  with  $A = 0.5$ ;  $Pr = 0.7$ ;  $\beta = 0.2$ ;  $\epsilon = 0.1$ ;  $R = 0.2$ ;  $\lambda = 0.2$ ;  $V_w = 0.424$ ;**